

# Real-Time Simulation of a Fully Detailed Type-IV Wind Turbine

O. Tremblay, R. Gagnon, M. Fecteau

**Abstract--** This paper presents an iterative nodal solver for power switching devices implemented in Hydro-Québec's real-time simulation software (Hypersim). The proposed algorithm, based on fixed-point iteration, combined with the latest supercomputer technology allows precise simulation of detailed switch models with an extra simulation cost per additional iteration of less than 25%. Real-time results for the full converter (type-IV) wind generator model, connected to a network equivalent through transformers and a collector system, show faster than real-time execution for a task containing many dozens of nodes and elements. Moreover, due to numerous natural commutation switches (as diodes), the iteration method is required to obtain results without numerical instability. The performances together with the precision of the simulation results show the efficiency of the new algorithm.

**Keywords:** Real-time simulation, voltage source converters (VSC), electromagnetic transient (EMT) simulation, wind generator model, type-IV, iteration solver, detailed converter.

## I. INTRODUCTION

THE massive integration of wind power plants (WPP) on transmission grids leads to new challenges for transient electromagnetic study of power systems. Hydro-Québec plans to integrate, by the end of 2015, 1000 MW of one of the most modern wind generator technologies: the full power converter wind generator (WG), or type-IV [1]. Since the dynamics of this system depends mainly on the converter control strategies, and each manufacturer has their own specificities, it is necessary to have a realistic control system and detailed converter representation in order to conduct precise electromagnetic studies on a real-time simulator.

Hydro-Québec's real-time simulator (Hypersim) is a large-scale multiprocessor simulator used for power system studies as well as for the development, validation, tuning and commissioning of control systems [2]. The computational effort is automatically spread across available processors using the natural propagation delay of the transmission lines. As a result, the large system impedance matrix is divided into several smaller submatrices which can be solved in parallel by many processors without introducing any error, thus drastically

increasing the simulation speed [3].

Electromagnetic transient (EMT) simulators typically use a piecewise linear representation of power electronic devices modeled as switches. The switches are turned on and off, depending on the control signals and the voltage-current conditions of the device, to synthesize the desired voltage. In order to better represent the harmonic behavior due to the pulse-width modulator (PWM), the simulation sampling frequency must be 50 to 100 times greater than the PWM carrier frequency [4]. The small simulation time step, in the order of a few microseconds, and the large matrix manipulations are very time-consuming in a real-time context [5]. To limit this overhead, the instantaneous change of natural commutation devices, caused by controlled switches or other nonlinear elements [6], is usually taken into account at the next simulation step. This approach is adequate for many cases but it can introduce numerical problems, particularly for the simulation of voltage-sourced converters (VSC) like the one in type-IV wind generators.

Many stratagems have been used over the years to overcome the heavy computational burden of switched networks [7]-[9]. These methods work well in normal operation but can introduce problems in abnormal conditions due to approximations of the switch behavior by inductance and/or capacitance or by voltage sources. These problems may include the behavior when the pulses are stopped, when dead time is applied on gate signals or when an AC or DC fault occurs near the converter. A detailed switch model combined with an iterative algorithm is sometimes necessary to get reliable simulation results.

Supercomputers now have sufficient processing power to provide the larger computational effort required by a real-time iteration engine for natural commutation devices. In order to fully exploit this new computational capability, Hypersim's simulation engine requires additional functionality.

This paper presents the implementation of a real-time iterative algorithm for natural commutation devices. The first section describes the new real-time iterative algorithm, based on fixed-point iteration, and its implementation in the nodal solver. A generic type-IV WG model, fully detailed converter topology and their associated control system containing a pulse width modulator (PWM) of 2 kHz are then presented. Results for a real-time, software-in-the-loop (SIL), simulation are furthermore presented: the type-IV converters are simulated in a real-time simulator and connected to a virtual generic controller simulated in a separate processor. The paper closes with a few concluding remarks.

---

O. Tremblay and R. Gagnon are with Hydro-Québec's Research Institute (IREQ), Réseaux électriques et mathématiques, 1800 Lionel-Boulet, Varennes, Qc, Canada, J3X 1S1 (e-mail of corresponding author: [tremblay.olivier@ireq.ca](mailto:tremblay.olivier@ireq.ca)).

M. Fecteau is with Hydro-Québec TransÉnergie, Études d'automatismes et protections.

## II. REAL-TIME ITERATIVE ALGORITHM

### A. Background

Hypersim uses nodal representation to simulate network elements. Using the trapezoidal integration technique (an A-stable numerical method), the dynamic elements are represented by a resistance in parallel with a current source, representing its history values. At each time step, the simulation engine calculates the node voltage with the following equation:

$$V = Y^{-1} \cdot I \quad (1)$$

where  $Y$ ,  $I$  and  $V$  are respectively the admittance matrix, the network sources and history injection, and lastly, the corresponding node voltage.

The switch elements are incorporated into the linear nodal solver using piecewise linear representation: the switch is represented by a small resistance when closed and by a large resistance when opened. Such discontinuous behavior often occurs with impulse voltage (when the current flowing through inductance changes abruptly) or impulse current (when the capacitor voltage suddenly changes). The precise detection of such impulses is critical because they may cause natural commutations in power electronic devices.

### B. Simple example: the buck converter

A simple circuit, the buck converter shown in Fig. 1, is used to illustrate the impact of the various circuit topologies.

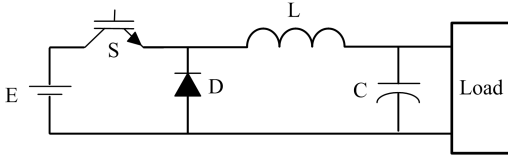


Fig. 1. Buck converter circuit.

In this circuit, containing two switches, four different topologies can occur:

1. At the beginning of a cycle, a pulse is applied to the IGBT ( $S = \text{on}$ ) and the diode is blocked ( $D = \text{off}$ ). The current increases through the inductance ( $L$ ) towards the load.
2. At a certain time, the pulse applied to the IGBT is removed ( $S = \text{off}$ ). At this time, the current flowing through the inductance ( $L$ ) tends to be interrupted since the diode is currently blocked.
3. The previous step will produce a voltage impulse that will appear across the diode, which will start to conduct instantaneously ( $D = \text{on}$ ).
4. When the pulse is applied again to the IGBT ( $S = \text{on}$ ), the voltage source is short-circuited, producing a negative current in the diode.

A negative current will immediately block the diode ( $D = \text{off}$ ) and the cycle restarts.

In practice, only two topologies can occur: steps 1 and 3

caused by the gate signal. Other topologies (2 and 4) are intermediate due to the natural commutations and need to be treated in an iterative process.

### C. Hypersim's new iterative nodal solver

The solver recalculates the node voltages for the entire substation at every state change of a switch device. Before the simulation starts, the admittance matrix is reordered to move down elements which may change their admittance contribution during the simulation (e.g., nonlinear elements and switches). This minimizes the time spent on re-factorization. Secondly, LDU decomposition and a forward-backward substitution are used to obtain the solution of node voltage during the simulation [10].

Figure 2 shows the new iterative engine implemented in Hypersim. At the beginning of a simulation step, the gate signal of each controllable switch is checked to decide whether a switch action is necessary. The contribution of the current sources to the node ( $I_{\text{node}}$ ) is determined before calculating the node voltage. The switch variables (voltage across and current flowing) are then updated according to the actual node voltage. If a switch changes their state (because of the actual node voltage), the new admittance contribution is updated before resolving the node voltage. This iterative process, called the fixed-point iteration, is pursued as long as required and can be limited by a maximum value to restrict the calculation time. The code generator has been optimized to concentrate the computational burden on iterative elements only. When the solution converges to the exact node voltage, element histories are updated in order to calculate the current injection  $I_{\text{node}}$  for the next time step.

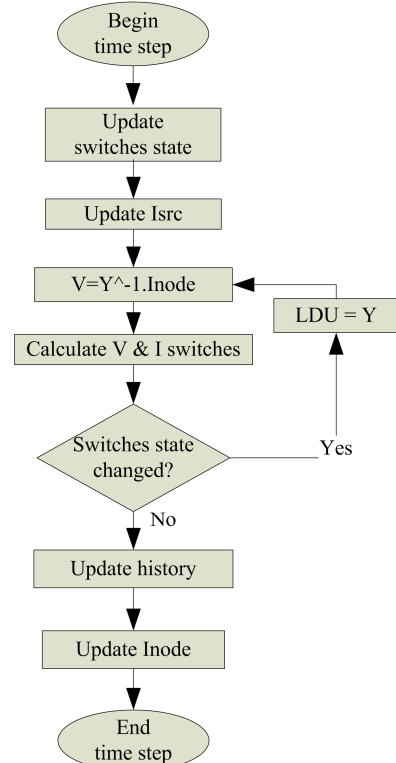


Fig. 2. Iterative engine flowchart.

#### D. Buck converter: simulation results

Figure 3 shows the simulation results (with a simulation time step of  $10 \mu\text{s}$ ) for the buck converter of section II.B, fed by a pulse generator operating at 2 kHz with a duty cycle of 50%. At the beginning of the simulation, the IGBT is closed and the current in the inductance starts to increase. After  $250 \mu\text{s}$ , the IGBT is opened and the diode should immediately close in a freewheeling mode. The number of maximum iterations is successively changed from 1 (no iteration) to 2. It is easy to observe that, without iteration, the diode is turned on only at the beginning of the next time step, introducing an undesirable state where the current in the inductance is suddenly stopped. As a result, major voltage instabilities cause the diode to successively open and close. When the maximum iteration number is increased to 2, the diode is immediately closed while the IGBT is turned off, as expected by the physical behavior. For this simple circuit, the maximum computation time is about  $1 \mu\text{s}$  for one iteration and increases by  $0.25 \mu\text{s}$  (25%) for two iterations.

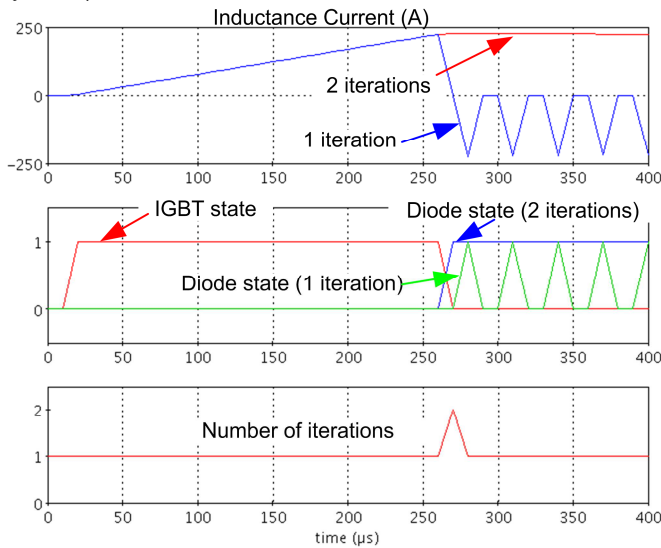


Fig. 3. Buck converter simulation results.

### III. TYPE-IV WIND GENERATOR MODEL

The wind generator with full power converter, or type-IV WG, shown in Fig. 4 represents one of the most modern technologies. The power captured by the wind turbine is transmitted to the drive train modeled as a two-mass system, while the mechanical power is converted to electrical power using a synchronous generator (SG). The pitch of the wind-turbine blades can be adjusted to maximize the power transfer and/or regulate the rotation speed.

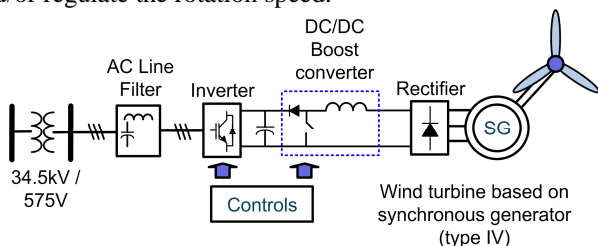


Fig. 4. Conceptual block diagram of the type-IV WG.

The particularity of this topology is the fact that the entire power of the synchronous generator goes through an AC/DC/AC power converter, allowing fast control of the active and reactive power delivered by the WG over a wide range of generator speeds. The power converters of this WG use fast power electronic devices, which support both firing and extinction control. This feature is used with PWM in the kHz range in order to synthesize the desired reference voltages. The rectifier contains six diodes while the inverter consists of six IGBT/diode pairs.

#### A. Generic Control System

The generic control system presented in this sub-section is based on public domain information and in-house expertise. The main control system, presented in Fig. 5, regulates the active and reactive power of the grid-side converter. The axis, used in the d-q transform, is aligned with the positive sequence of the grid voltage, using a phase-locked loop.

The active power is controlled indirectly by regulating the DC bus voltage. An increase in the bus voltage means that more energy comes from the WG. In order to extract this additional energy, the desired active current ( $I_{d\text{ref}}$ ) of the grid is augmented to reduce the DC bus voltage close to the desired value. Inversely, when the DC bus voltage is lower than the expected value, the WG extracts less energy from the wind. As a result, the desired active current ( $I_{d\text{ref}}$ ) is reduced.

The reactive power is controlled by a “var” regulator, providing the grid terminal voltage reference ( $V_{\text{ref}}$ ). The reactive power reference ( $Q_{\text{ref}}$ ) comes from the wind farm control system (not described in this paper). The actual voltage magnitude is compared to its reference and the voltage error is reduced to zero by a voltage integral regulator, providing the desired grid reactive current ( $I_{q\text{ref}}$ ).

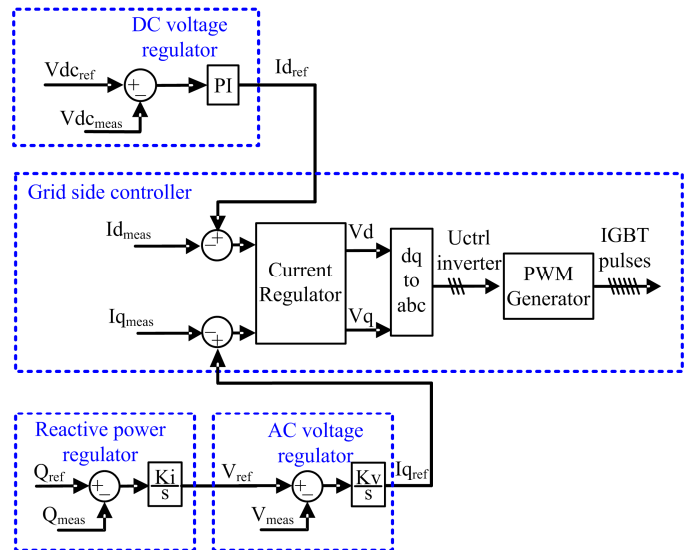


Fig. 5. Main controller.

The measured currents ( $I_{d\text{meas}}$ ,  $I_{q\text{meas}}$ ) are compared to the references ( $I_{d\text{ref}}$ ,  $I_{q\text{ref}}$ ) and the error is minimized using two PI regulators and a well known decoupling feed-forward

technique in order to calculate the desired AC voltage in the dq reference frame (Vdq). A dq-abc transformation followed by a PWM generator produces the pulses for the 2-level VSC.

Finally, the wind turbine controllers contain (Fig. 6) a speed regulator and a pitch controller designed to extract the maximum wind power. The former is achieved with two cascaded PI regulators: The first controller uses the speed error to determine the desired DC current ( $I_{dc\_ref}$ ) and the second regulates the current flowing through the inductance by modifying the duty cycle of the DC/DC converter. As a result, the current extracted from the synchronous generator (via the diode rectifier) will be affected and consequently, the wind turbine speed via the electromagnetic torque.

Meanwhile, the pitch controller modifies the pitch angle to limit the extracted power to its rated value. In this implementation, a pitch angle of  $0^\circ$  corresponds to maximum wind power extraction. This means that under strong wind conditions, the pitch angle is increased leading to unexploited or lost wind energy, in order to respect operation ratings.

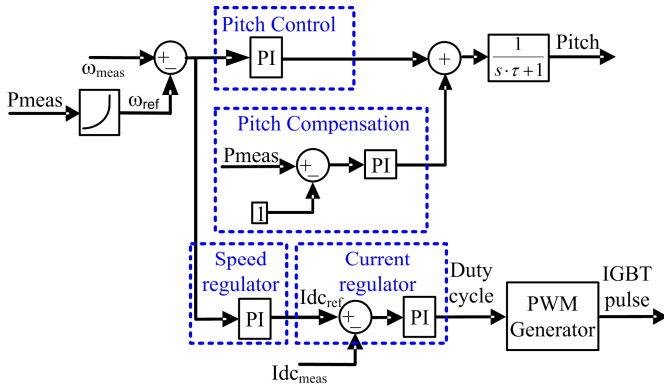


Fig. 6. Wind turbine controllers: Speed regulator and Pitch control.

#### IV. REAL-TIME SIMULATION

Hydro-Québec needs a detailed EMT representation of the wind generator to study control-type interaction between many

WPPs, real HVDC controllers and real static var compensator (SVC) controllers simulated in real-time. Furthermore, a fully detailed representation of the power converter is required to verify the effect of voltage transients on the transmission system during and after a network event, in particular when the pulses are stopped.

The purpose of this study is to connect a generic virtual control system to an aggregated WG model [11]-[13]. In the future, it is planned to work together with WG manufacturers on vendor-specific models in order to incorporate the virtual controllers (in a black box form) into Hypersim. For the test case shown below, the generic control system of section III.A is used and modeled in Simulink. Apart from the DC bus overvoltage (crow bar), complex protection schemes are not implemented in this control system. A 2 kHz switching frequency is used for the inverter PWM and the DC/DC converter pulse generator.

Figure 7 shows the real-time implementation of a 2-MW (with a power factor of 0.9) type-IV WG. The power system, consisting of the network equivalent of 67 MVA at 120 kV, the station transformer and grounding system, the equivalent collector system for one WG, the WG transformer, the power converters and the synchronous generator, is simulated in one CPU at a 10- $\mu$ s time step. The electrical values of the system are presented in Table I.

The control system, comprising the main controller, the WG controllers and the excitation regulator, is simulated by another CPU at the same sampling time. The C code of the control system is generated by the Simulink coder and integrated in the real-time simulation via an interface called Hyperlink.

A constant wind speed applied to the wind turbine system, allows an active power of about 2 MW to be extracted. The desired reactive power is set at 0 Mvar. Figure 8 shows, from 0 s to 0.05 s, the steady-state results for the DC bus voltage, the AC currents, the active and reactive power, the machine speed, the pitch angle and the number of iterations needed to procure

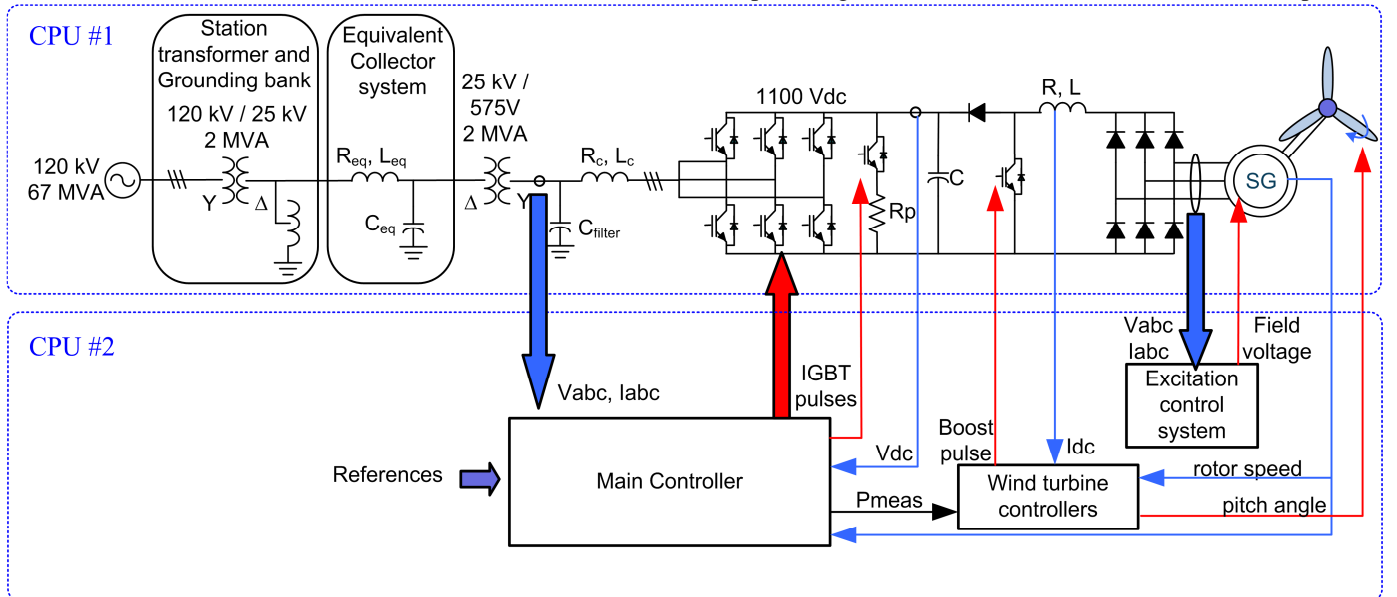


Fig. 7. Wind turbine controllers: Speed regulator and Pitch control.

the exact switch topologies.

TABLE I  
POWER SYSTEM PARAMETERS

Parameters	Values
Network equivalent	120 kV, Short-circuit level: 67 MVA
Station transformer	120 kV / 25 kV, 2.2 MVA R = .00266 pu, L = 0.08 pu
Equivalent collector system	Req = 0.016 pu, Xeq = 0.059 pu Beq = 0.032 pu
Wind turbine transformer	25 kV / 575 V, 2.2 MVA Rc = .0016 pu, Lc = 0.05 pu Cfilter = 150 kVar (Q = 50)
Converter	Protection resistance : Rp = 0.6 Ω DC bus capacitor : C = 90 mF Boost inductance: L = 120 μH (R = 0.5 mΩ)
SG	730 V, 2.2 MVA

It may be observed that the pitch controller works adequately to maintain the SG at its nominal speed (1 pu). For this wind turbine, a 12-m/s wind speed corresponds to the nominal power (2 MW) with a pitch angle of about 3.2°. The DC bus regulator keeps the bus voltage at its nominal value of 1100 V with low ripple. Finally, the active and reactive power follow their reference values.

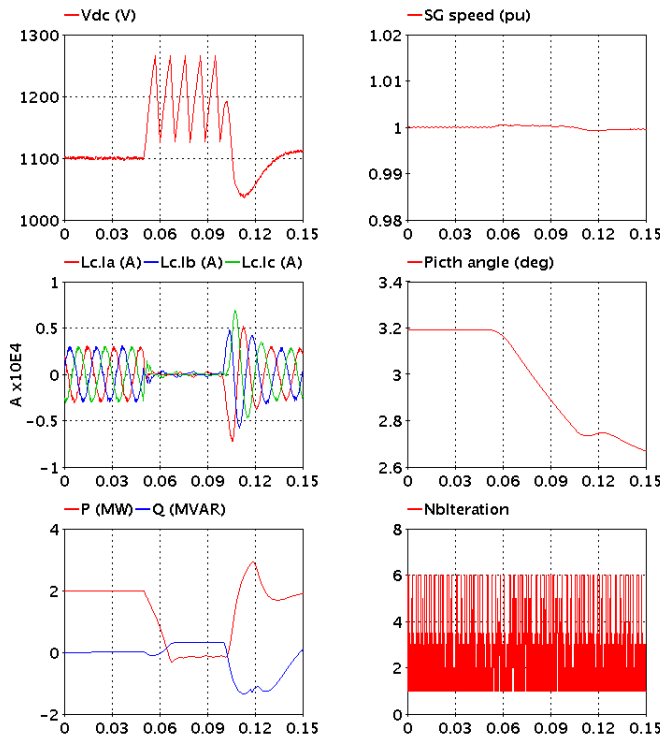


Fig. 8. Real-time simulation results.

When a network event occurs (in this case an overvoltage of 1.5 pu during 3 cycles) the main controller can hypothetically stop the pulses sent to the IGBTs. At this time (t

= 0.05 s), it is essential to represent the exact switch behavior (high impedance when the IGBT/diode pairs are open or diode mode when overvoltage occurs), to study the system recovery dynamics. During the event, three phenomena can be studied (Fig. 9): firstly, the bridge acts as an open circuit for 1 ms. Secondly, during this time, the SG contributes to an increase in the bus voltage because it continues to feed the system. Finally, the overvoltage causes the IGBT/diodes bridges to act as a Graetz bridge which also increases the DC bus voltage. The latter rises to a threshold value and enables a protection mode, where the extra energy is burned into the resistor Rp. It is also possible to observe slight diode bouncing when the voltage and current conditions are close to the threshold values. When the system restarts, the system recovery dynamics can be studied.

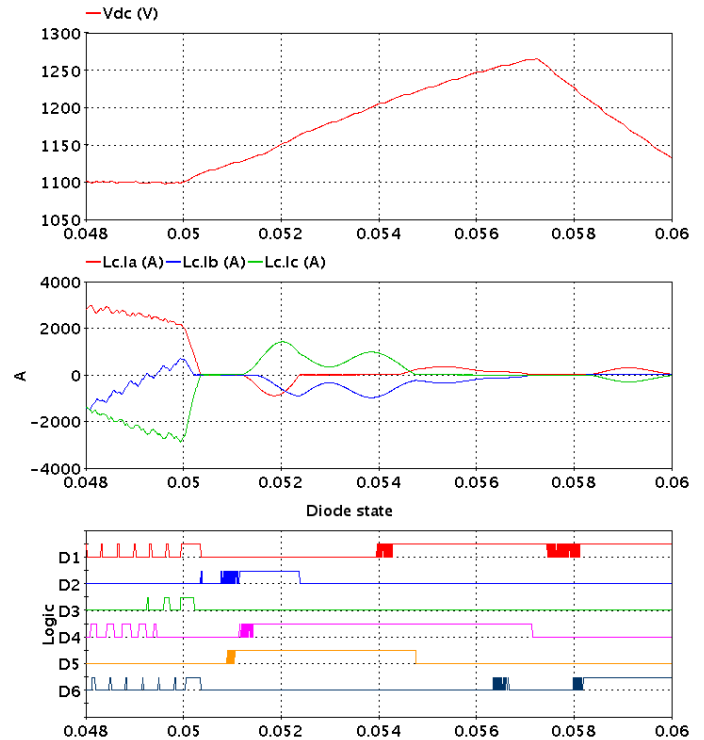


Fig. 9. Real-time simulation results (zoom).

Table II shows the number of elements simulated by the two CPUs. During the whole simulation, a maximum of six iterations are needed to compute the exact switch topology. Nevertheless, the execution time is kept below the 10-μs real-time constraint. It can be noted that without the iterative process on natural commutation switches, it is impossible to get precise results due to the lack of instantaneous diode commutation in the IGBT/diode pairs. The results begin to be acceptable with three iterations, resulting in an execution time

TABLE II  
REAL-TIME SIMULATION PERFORMANCES

CPU	NB	CONTROL SYSTEM						Analog comm.	Execution time
		Nodes	Transformers	Passives	Sources	Switches	Digital comm.		
1	37	9	46	6	15	8-in	15-out / 2-in	5.8 μs (3 iterations) 6.7 μs (4 iterations) 7.9 μs (5 iterations) 8.8 μs (6 iterations)	
2						8-out	15-in / 2-out	7.5 μs	

of 5.8  $\mu\text{s}$ . Each additional iteration, resulting in better accuracy, increases the execution time by about 1  $\mu\text{s}$ . The iteration process, even for this heavy computation task, increases the execution time by no more than 15%, confirming the efficiency of the implementation in the real-time nodal solver.

## V. CONCLUSIONS

This paper has demonstrated the efficiency of the new iterative engine implemented in the real-time simulator Hypersim. A simple case study illustrates the need for an iterative process to accurately represent natural commutations in the devices. The new nodal iterative solver based on fixed-point iteration was introduced. Optimization of the real-time code generator now makes it possible to concentrate the calculation burden on the iterative elements only. A generic type-IV wind generator model associated with its control system is presented. Real-time simulation, with the generic virtual controller, proves that it is essential to represent the detailed model of the electronic switches to study the system behavior in abnormal conditions. With the new iteration engine, this network can be simulated without numerical instabilities, thereby increasing the reliability and precision of the results. The computation time is less than the real-time constraint imposed by the calculation step, even when many iterations are required to converge to the exact solution.

## VI. REFERENCES

- [1] R. Gagnon, M. Fecteau, P. Prud'Homme, E. Lemieux, G. Turmel, D. Paré, F. Duong. "Hydro-Québec Strategy to Evaluate Electrical Transients Following Wind Power Plant Integration in the Gaspésie Transmissions System" *IEEE Transactions on Sustainable Energy*, Vol. 3, No. 4, pp. 880-889, Oct. 2012.
- [2] V. Q. Do, J.-C. Soumagne, G. Sybille, G. Turmel, P. Giroux, G. Cloutier, S. Poulin. "Hypersim, an Integrated Real-Time Simulator for Power Networks and Control Systems" *ICDS'99*, Vasteras, Sweden, May 1999, pp.1-6.
- [3] D. Paré, G. Turmel, J.-C. Soumagne, V. A. Do, S. Casoria, M. Bissonnette, B. Marcoux, D. McNabb. "Validation tests of the Hypersim digital real time simulator with a large AC-DC network" *Proc. of the International Conference on Power Systems Transients, IPST'2003*, New Orleans, LA, Sept. 28 to Oct. 2, 2003, pp. 577-582.
- [4] Wei Li; Joos, G.; Belanger, J.; , "Real-Time Simulation of a Wind Turbine Generator Coupled With a Battery Supercapacitor Energy Storage System," *IEEE Transactions on Industrial Electronics*, vol.57, no.4, pp.1137-1145, April 2010.
- [5] R. Gagnon, G. Turmel, C. Larose, J. Brochu, G. Sybille, M. Fecteau, "Large-Scale Real-Time Simulation of Wind Power Plants into Hydro-Québec Power System," in *Proc. WIW'10*, Québec, Canada, Oct. 2010, pp. 472-478.
- [6] O. Tremblay, M. Fecteau, P. Prud'Homme "Precise Algorithm for Nonlinear Elements in Large-Scale Real-Time Simulator," in *Proc. of the CIGRÉ Canada Conf. on Power Systems*, Montréal, Canada, Sept. 2012.
- [7] T.L. Maguire and W.J. Giesbrecht, "Small Time-Step (<2 $\mu\text{Sec}$ ) VSC Model for the Real Time Digital Simulator" in *Proc. IPST 2005*, Montreal Canada, June 2005, Paper No. IPST05-168-25c.
- [8] C. Dufour, J. Belanger, "Discrete Time Compensation of Switching Events for Accurate Real-Time Simulation of Power Systems", *Proc. of the IEEE 27th Industrial Electronics Society Conference (IECON-01)* , Vol. 2, Nov.-Dec. 2001, p.1533-1538.
- [9] M. Harakawa, H. Yamasaki, T. Nagano, S. Abourida, C. Dufour and J. Bélanger, "Real-Time Simulation of a Complete PMSM Drive at 10  $\mu\text{s}$  Time Step", *Proc. of the 2005 International Power Electronics Conference (IPEC-Niigata 2005)* – Niigata, Japan, April 4-8, 2005.
- [10] V.Q. Do, D. McCallum, P. Giroux, B. De Kelper. "A backward-forward interpolation technique for a precise modelling of power electronic in HYPERSIM" *Proc. of the International Conference on Power Systems Transients, IPST'2001*, Rio de Janeiro, Brazil, June 2001.
- [11] J. Brochu, C. Larose and R. Gagnon, "Validation of single- and multiple-machine equivalents for modeling wind power plants," *IEEE Trans. Energy Conversion*, vol. 26, pp. 532-541, June 2011.
- [12] E. Muljadi, C. P. Butterfield, A. Ellis, J. Mechenbier, J. Hochheimer, R. Young, N. Miller, R. Delmerico, R. Zavadil and J.C. Smith, "Equivalent the collector system of a large wind power plant," *IEEE Power Eng. Soc. Gen. Meeting*, Montreal, Canada, June 18-22, 2006.
- [13] E. Muljadi, S.Pasupulati, A. Ellis and D. Kosterov, "Method of equivalent for a large wind power plant with multiple turbine representation," *IEEE Power&Energy Soc. Gen. Meeting Conv.&Delivery of Elect. Energy in the 21st Century*, July 20-24, 2008.